

# Dynamical QCD Predictions for Ultrahigh Energy Neutrino Cross Sections

M. Glück, S. Kretzer and E. Reya

Institut für Physik, Universität Dortmund  
D-44221 Dortmund, Germany

## Abstract

Neutrino-nucleon total cross sections for neutrino energies up to ultrahigh energies (UHE),  $E_\nu = 10^{12}$  GeV, are evaluated within the framework of the dynamical (radiative) parton model. The expected uncertainties of these predictions do not exceed the level of about 20 % at the highest energies where contributions of parton distributions in the yet unmeasured region around  $x \simeq 10^{-8}$  to  $10^{-9}$  are non-negligible. This is far more accurate than estimated uncertainties of about  $2^{\pm 1}$  due to ad hoc extrapolations of parton distributions to  $x < 10^{-5}$  required for calculating UHE cosmic neutrino event rates.

Calculations of ultrahigh-energy (UHE) neutrino-nucleon total cross sections, relevant for neutrino astronomy, have been improved [1, 2, 3, 4] by taking into account new high energy measurements of deep inelastic lepton-nucleon scattering (DIS) at DESY-HERA [5]. These updated calculations were even further improved very recently [6] not only due to additional small- $x$  precision measurements at HERA [7] which became available in the meantime, but mainly due to new ideas about the flux of neutrinos [8] from active galactic nuclei (AGNs) [9], gamma ray bursts (GRBs) [10] or from decays of exotic heavy particles of generic top-down (TD) or topological defects models [11]. Most of these new developments refer to neutrino energies above about  $10^8$  GeV where (anti)neutrino-nucleon cross sections become sensitive to parton densities at ultrasmall values of Bjorken- $x$ ,  $x < 10^{-5}$ , not accessible by present DIS experiments. Different *assumptions* about the  $x \rightarrow 0$  behavior then lead to different cross sections. Thus a significant uncertainty in estimating the detectability of extraterrestrial UHE neutrinos with present and future neutrino telescopes is due to the small- $x$  extrapolations and the resulting uncertainty reaches typically a factor  $2^{\pm 1}$  around  $10^{20}$  eV [2, 6].

The highest presently available  $ep$  energy at HERA,  $\sqrt{s_{ep}} = 314$  GeV, is rather small as compared to the envisaged UHE neutrino nucleon collision energies of up to about  $\sqrt{s_{\nu N}} = 10^6$  GeV. Estimates of the corresponding total  $\bar{\nu} N$  cross sections thus afford either extensive, possibly unreliable, extrapolations [1, 2, 3, 4, 6] of existing data ( $x \gtrsim 10^{-5}$ ) and their respective fits, or the application [3] of QCD inspired models which proved to provide reliable high energy predictions [12, 13, 14] in the past [5, 7]. In the present work we shall adopt this second option and base our predictions on calculations within the framework of the radiative parton model [12, 13, 14, 15] which allows to calculate the small- $x$  ( $x \lesssim 10^{-2}$ ) behavior of parton densities from first principles, i.e. QCD dynamics, independently of any free (fit) parameters in the small- $x$  region. These unique dynamical predictions result from valence-like gluon and sea input densities  $xg(x, Q_0^2) \sim x^a$ ,  $x\bar{q}(x, Q_0^2) \sim x^{a'}$  with  $a, a' > 0$  as  $x \rightarrow 0$  at some low momentum scale  $Q_0 \simeq 0.5 - 0.6$  GeV. The resulting small- $x$  behavior is furthermore perturbatively stable and unique at the relevant momentum scales  $Q^2 \simeq M_W^2$ . Here we shall apply the parton distributions in [14], and in

particular the most recent ones in [15] which take also into account all recent high precision measurements at HERA [7, 16], to evaluate  $\sigma^{(\bar{\nu})N}(E_{(\bar{\nu})})$  for  $10^2 \lesssim E_{(\bar{\nu})} \lesssim 10^{12}$  GeV. At highest neutrino energies, this requires the knowledge of parton densities down to  $x \simeq 10^{-8}$  ( $x \gtrsim M_W^2/2ME_\nu$  due to the  $W$ -propagator, with  $M$  being the nucleon mass) at scales  $Q^2 \simeq M_W^2$ . In ref. [15] we have explicitly demonstrated that our next-to-leading order (NLO) results in this extremely small- $x$  region are perturbatively stable when compared with the leading order (LO) ones. It should be kept in mind that this stability refers always to measurable quantities like structure functions or cross sections rather than to the auxiliary, not directly measurable, NLO parton distributions [14, 15] since perturbative stability usually requires  $f^{NLO}(x, Q^2) \neq f^{LO}(x, Q^2)$  for  $f = q, \bar{q}, g$ . Furthermore, the NLO predictions are, in contrast to the LO ones, obviously rather insensitive to the specific choice for the renormalization scale  $\mu_R$  appearing in  $\alpha_s(\mu_R^2)$  and for the factorization scale  $\mu_F$  appearing in the parton densities  $f(x, \mu_F^2)$  [15]. We shall therefore mainly concentrate on NLO analyses for predicting the various UHE total cross sections relevant for neutrino astronomy.

The above results lend sufficient confidence in the reliability of the perturbatively calculated UHE  $(\bar{\nu})^N$  total cross sections,  $N = (p + n)/2$ , evaluated according to

$$\sigma^{(\bar{\nu})N}(s) = \int_0^1 dx \int_0^1 dy \, d^2\sigma^{(\bar{\nu})N}/dxdy \quad (1)$$

with

$$\frac{d^2\sigma^{(\bar{\nu})N}}{dxdy} = \frac{G_F^2 s}{2\pi} (1 + xys/M_W^2)^{-2} [(1-y)F_2^{(\bar{\nu})} + y^2 x F_1^{(\bar{\nu})} \pm y(1 - \frac{y}{2})x F_3^{(\bar{\nu})}] \quad (2)$$

where  $F_i = F_i(x, Q^2 = xys)$ ,  $s = 2ME_{(\bar{\nu})}$  and  $G_F = 1.1663 \times 10^{-5}$  GeV $^{-2}$ . It should be noted that the results for the total cross sections are insensitive to the lower integration limits in (1) since the  $W$ -propagator in (2) restricts  $Q^2 = xys$  to values around  $M_W^2$ . Anyway, as soon as the integrations correspond to scales  $Q^2 < Q_0^2$ , we freeze the respective parton densities at their given input scale  $Q^2 = Q_0^2$ . The  $(\bar{\nu})^N$  structure functions  $F_i$  in (2) can be decomposed as

$$F_i = F_i^{light} + F_i^h \quad (3)$$

where  $F_i^{light}$  refers to all light ( $u, d, s$ ) contributions and  $F_i^h$  denotes all relevant contributions related to heavy quark ( $c, b, t$ ) transitions.

For charged current (CC)  $\nu_l N \rightarrow l^- X$  reactions we have in LO-QCD

$$\begin{aligned} F_1^{\nu, light} &= \frac{1}{2}(\bar{u} + \bar{d}) + \frac{1}{2}(d + u)|V_{ud}|^2 + s|V_{us}|^2 \\ F_2^{\nu, light} &= 2xF_1^{\nu, light} \\ F_3^{\nu, light} &= -(\bar{u} + \bar{d}) + (d + u)|V_{ud}|^2 + 2s|V_{us}|^2 \end{aligned} \quad (4)$$

where  $u = u(x, Q^2)$  etc., except stated otherwise,  $s = \bar{s}$  and the CKM mixing matrix elements are taken from [17]. The heavy flavor component  $F_i^h$  in LO consists of the charm contribution  $F_i^c$  according to the  $W^+s \rightarrow c$  and  $W^+d \rightarrow c$  transitions as described, for example, in [18], and of the top-bottom contribution  $F_i^{t\bar{b}}$  according to the  $W^+g \rightarrow t\bar{b}$  fusion subprocess [19], using a factorization and renormalization scale equal to  $(m_t + m_b)$  with  $m_t = 175$  GeV and  $m_b = 4.5$  GeV. [Note that the sign convention for  $F_3$  in [19] is opposite to the one in eq. (2)]. We shall compare these heavy quark contributions also with the less adequate, but frequently used (e.g., [1, 2, 3, 4, 6]) massless approach (the so called 'variable flavor' scheme) where intrinsic 'heavy' quark densities are purely radiatively generated using the ordinary massless evolution equations, starting at  $Q = m_h$ . In this case,  $F_i^h(x, Q^2)$  in (3) is given by

$$\begin{aligned} F_1^{\nu, h} &= \frac{1}{2}(d + u)|V_{cd}|^2 + s|V_{cs}|^2 + c + b(\xi, Q^2 + m_t^2)|V_{tb}|^2 \\ F_2^{\nu, h} &= x(d + u)|V_{cd}|^2 + 2xs|V_{cs}|^2 + 2xc + 2\xi b(\xi, Q^2 + m_t^2)|V_{tb}|^2 \\ F_3^{\nu, h} &= (d + u)|V_{cd}|^2 + 2s|V_{cs}|^2 - 2c + 2b(\xi, Q^2 + m_t^2)|V_{tb}|^2 \end{aligned} \quad (5)$$

with  $\xi = x(1 + m_t^2/Q^2)$  and where we neglected  $m_c^2/Q^2$  contributions as well as  $t(x, Q^2)$ . We choose the scale  $Q^2 + m_t^2$  in  $b$ , since it resulted in the best perturbative LO/NLO stability in the  $c\bar{s}$  sector [18]. For this latter analysis in the so called 'variable flavor' scheme we shall use the dynamical parton densities of ref. [13]. The relevant structure functions for CC  $\bar{\nu}N$  reactions in (2) are simply obtained from the above expressions via  $F_{1,2}^{\bar{\nu}} = F_{1,2}^{\nu}(q \leftrightarrow \bar{q})$  and  $F_3^{\bar{\nu}} = -F_3^{\nu}(q \leftrightarrow \bar{q})$ .

In NLO-QCD all above LO parton densities have to be replaced by the NLO ones [14, 15], with the appropriate addition of convolutions with the fermionic Wilson coefficient  $C_q$  and the NLO contribution  $C_g \otimes g$ , as summarized for example in [20]. It turns out that these additional convolutions contribute less than about 2% and thus these complications can be safely neglected for NLO calculations of high-energy total  $\nu^{(-)} N$  cross sections. The heavy flavor piece  $F_i^h$  receives additional massive  $\mathcal{O}(\alpha_s)$  contributions according to the  $W^+g \rightarrow c\bar{s}$ ,  $W^+s' \rightarrow gc$ , etc., subprocesses [18, 21, 22] which we include according to the  $(\overline{\text{MS}})$  results of [18]. The fact that the  $t\bar{b}$  production has so far only been calculated in LO ( $W^+g \rightarrow t\bar{b}$ ) is of minor importance, since the  $c\bar{s}$  sector dominates over the much heavier  $t\bar{b}$  one. It should be noted that this more appropriate way of calculating the heavy quark contributions in fixed order perturbation theory without neglecting mass effects, usually referred to as 'fixed flavor' factorization scheme (also adopted in [14, 15]), results in perturbatively stable LO/NLO QCD-predictions [18] even for the highest energies [23] attainable with present cosmic ray shower experiments ( $\sqrt{s} = 10^4 - 10^5$  GeV).

For completeness we also summarize briefly the structure functions in (2) for neutral current (NC) reactions, where obviously  $M_W \rightarrow M_Z$ . For  $\nu N \rightarrow \nu X$  the light quark contributions in LO are

$$\begin{aligned} 2F_1^{\nu,light} &= \frac{1}{2}(u + \bar{u} + d + \bar{d})(V_u^2 + A_u^2) + \frac{1}{2}(u + \bar{u} + d + \bar{d} + 4s)(V_d^2 + A_d^2) \\ F_2^{\nu,light} &= 2xF_1^{\nu,light} \\ 2F_3^{\nu,light} &= 2(u_v + d_v)(V_u A_u + V_d A_d) \end{aligned} \tag{6}$$

where  $q_v = q_v(x, Q^2) \equiv q - \bar{q}$  and  $V_u = \frac{1}{2} - \frac{4}{3}\sin^2\theta_W$ ,  $V_d = -\frac{1}{2} + \frac{2}{3}\sin^2\theta_W$ ,  $A_u = -A_d = \frac{1}{2}$  with  $\sin^2\theta_W = 0.232$ . The (massive) heavy flavor contributions to  $F_{1,2}^{\nu,h}$  derive from the subprocesses  $Z^0g \rightarrow h\bar{h}$ ,  $h = c, b$  and are given in [19], with  $F_3^{\nu,h} = 0$ . (The small contribution from  $t\bar{t}$  production will be neglected). If heavy quarks are treated less adequately as massless intrinsic partons, we have instead of eq. (5),

$$\begin{aligned} 2F_1^{\nu,h} &= 2c(V_u^2 + A_u^2) + 2b(V_d^2 + A_d^2) \\ F_2^{\nu,h} &= 2x F_1^{\nu,h} \quad , \quad F_3^{\nu,h} = 0 \quad . \end{aligned} \tag{7}$$

In this massless case,  $c = c(x, Q^2)$  etc., we use again the 'variable flavor' parton densities of ref. [13]. For NC  $\bar{\nu}N \rightarrow \bar{\nu}X$  reactions, one simply has  $F_i^{\bar{\nu}} = F_i^{\nu}$ . In NLO all above LO parton distributions have to be replaced by the NLO ones [14, 15], with the additional convolutions  $C_q \otimes q$  and  $C_g \otimes g$  [20] being again negligible as for CC reactions.<sup>1</sup>

Our relevant most recent NLO( $\overline{\text{MS}}$ ) sea and gluon densities [15] at  $Q^2 = M_W^2$  are shown in fig. 1, where they are also compared with our previous GRV 94 [14] predictions<sup>2</sup> which are slightly steeper for  $x < 10^{-5}$ , relevant for  $\nu N$  cross sections at  $E_\nu > 10^8$  GeV. For illustration we also show the input of the valence-like NLO GRV 98 densities at the input scale  $Q_0^2 = 0.40 \text{ GeV}^2$  which becomes vanishingly small at  $x < 10^{-2}$ , particularly for the gluon input. This illustrates the purely dynamical (i.e. parameter-free) origin of the very small- $x$  structure of sea quark densities and in particular of the gluon density at  $Q^2 > Q_0^2$  which dominates the  $Q^2$  evolution of  $\bar{q}(x, Q^2)$  in the small- $x$  region. Also noteworthy is the stability of  $\bar{u} + \bar{d}$  at  $Q^2 = M_W^2 \gg Q_0^2$  with respect to our previous GRV 94 results. For comparison the expectations based on the CTEQ3-DIS [24] and CTEQ4-DIS [25] parton densities<sup>3</sup> are shown as well. Whereas the CTEQ3 extrapolations seem to overestimate the very small- $x$  region,  $x < 10^{-5}$ , the CTEQ4 ones are in reasonable agreement with our dynamical expectations.

The resulting CC total  $\nu N$  cross sections are presented in fig. 2 which demonstrates the stability of the QCD predicted cross sections in the UHE region. The heavy quark contributions are also shown separately: The  $cs'$  sector contributes significantly, whereas

---

<sup>1</sup> Since the fully massive NLO contributions to  $Z^0 g \rightarrow h\bar{h}$  have not yet been calculated, we use the  $\text{LO}(\alpha_s)$  expressions for the NLO analysis as well. (The factorization scale is taken to be  $\mu_F^2 = 4m_h^2$  which provides the best perturbative LO/NLO stability for photon-induced processes  $\gamma^* g \rightarrow h\bar{h}$ , etc. [23] – a stability which holds down to  $x = 10^{-8}$ ). The same holds for the above CC contribution due to  $W^+ g \rightarrow t\bar{b}$ . This approximation is of minor importance, since the main contributions come, in both CC and NC cases, from the perturbatively stable light  $u, d, s$  quarks and the  $c\bar{s}$  sector.

<sup>2</sup> The simple analytic parametrizations of the LO and NLO QCD-evolution GRV 94 predictions for parton densities presented in [14] are sufficiently accurate down to the lowest relevant  $x \simeq 10^{-8}$ . Moreover, the NLO(DIS) results are practically the same as the NLO ( $\overline{\text{MS}}$ ) ones for GRV 94 [14] as well as for the more recent GRV 98 [15] distributions.

<sup>3</sup> These densities have been extrapolated to low- $x$  ( $x \lesssim 10^{-5}$ ) beyond the validity of the fitted parametrizations ( $x > 10^{-5}$ ) using some reasonable analytic functions. As in the case of the CTEQ3 densities [24], the CTEQ collaboration provided us with similar extrapolation functions for the CTEQ4 distributions [25]. We thank Wu-Ki Tung for a helpful correspondence.

the much heavier  $t\bar{b}$  contribution is small. These exactly calculated massive results are also compared with the results obtained from the less adequate description of treating heavy quarks as massless intrinsic partons according to eq. (5), using the GRV 92 densities [13]. Although this latter simplified massless approach to 'heavy' quark effects *overestimates* their contributions, their difference with respect to the exact massive treatment becomes rather marginal at scales as large as  $Q^2 \simeq M_W^2$ . It should be mentioned that in practically all conventional approaches where parton densities are obtained from fitting appropriate parametrizations to presently available DIS data, to be discussed below, heavy quarks are treated as massless intrinsic partons. This is also the case for the GQRS 98 results [6] shown in fig. 2 which are based on the CTEQ4-DIS parton distributions as the nominal distributions for calculating neutrino-nucleon cross sections and estimating astrophysical UHE neutrino event rates. It should be kept in mind that these results have been obtained by using some ad hoc 'brute force' extrapolation to  $x < 10^{-5}$ , i.e. by extrapolating the CTEQ4-DIS densities below  $x = 10^{-5}$  with the *same* power in  $x$  predicted at  $x = 10^{-5}$  and  $Q^2 = M_W^2$  [6]<sup>4</sup>. This overestimates the light sea quark densities at  $x \simeq 10^{-8}$  by almost 20% as compared to the CTEQ extrapolations [25]<sup>3</sup> shown in fig. 1 and thus also overestimates the cross section by the same amount at  $E_\nu \simeq 10^{12}$  GeV. Nevertheless, the expected total cross sections agree, somewhat accidentally, rather well with our dynamical predictions and are thus perfectly legitimate for practical applications.

To test the amount of extrapolation in  $x$  and  $Q^2$  involved in these calculations of total cross sections, fig. 3 shows the contribution to  $\sigma_{CC}^{\nu N}$  from different regions of  $x$ , i.e. by choosing a finite lower limit of  $x$ -integration  $x \geq x_{min}$  in eq. (1): Even at highest neutrino energies the  $W$ -propagator in (2) constrains [1, 2] the relevant values of  $x$  to be larger than about  $10^{-9}$ . For similar reasons the relevant  $Q^2$  is restricted to values near  $M_W^2$  for  $E_\nu \gtrsim 1$  TeV. Since our dynamical QCD small- $x$  predictions for  $x \lesssim 10^{-2}$  agree with all present DESY-HERA measurements down to  $x \simeq 10^{-5}$ , as discussed at the beginning, our dynamical predictions for UHE  $\nu(\bar{\nu})$  nucleon cross sections, which are dominated by  $x \gtrsim 10^{-8} - 10^{-9}$ , appear to be reasonably reliable.

---

<sup>4</sup> We thank Ina Sarcevic for a clarifying correspondence on this point.

Similar results hold for  $CC \bar{\nu}N$  and for the NC  $\nu(\bar{\nu})N$  total cross sections. Our final dynamical NLO high energy (small- $x$ ) predictions, based on our GRV 98 parton distributions [15], are given within 5 to 10% by

$$\begin{aligned}\sigma_{CC}^{\nu N} &= \begin{cases} 1.10 \times 10^{-36} \text{cm}^2 (E_\nu/1\text{GeV})^{0.454} & , 10^5 \lesssim E_\nu \lesssim 10^8 \text{GeV} \\ 5.20 \times 10^{-36} \text{cm}^2 (E_\nu/1\text{GeV})^{0.372} & , 10^8 \lesssim E_\nu \lesssim 10^{12} \text{GeV} \end{cases} \\ \sigma_{CC}^{\bar{\nu}N} &= \begin{cases} 6.65 \times 10^{-37} \text{cm}^2 (E_{\bar{\nu}}/1\text{GeV})^{0.484} & , 10^5 \lesssim E_{\bar{\nu}} \lesssim 10^8 \text{GeV} \\ 5.20 \times 10^{-36} \text{cm}^2 (E_{\bar{\nu}}/1\text{GeV})^{0.372} & , 10^8 \lesssim E_{\bar{\nu}} \lesssim 10^{12} \text{GeV} \end{cases} \\ \sigma_{NC}^{\nu N} &= \begin{cases} 3.55 \times 10^{-37} \text{cm}^2 (E_\nu/1\text{GeV})^{0.467} & , 10^5 \lesssim E_\nu \lesssim 10^8 \text{GeV} \\ 3.14 \times 10^{-36} \text{cm}^2 (E_\nu/1\text{GeV})^{0.349} & , 10^8 \lesssim E_\nu \lesssim 10^{12} \text{GeV} \end{cases} \\ \sigma_{NC}^{\bar{\nu}N} &= \begin{cases} 3.04 \times 10^{-37} \text{cm}^2 (E_{\bar{\nu}}/1\text{GeV})^{0.474} & , 10^5 \lesssim E_{\bar{\nu}} \lesssim 10^8 \text{GeV} \\ 3.14 \times 10^{-36} \text{cm}^2 (E_{\bar{\nu}}/1\text{GeV})^{0.349} & , 10^8 \lesssim E_{\bar{\nu}} \lesssim 10^{12} \text{GeV} \end{cases} .\end{aligned}$$

In fig. 4 we compare our most recent predictions for  $\sigma_{CC}^{\nu N}$  as a representative example, based on the GRV 98 distributions, with calculations based on different sets of parton densities and small- $x$  extrapolations. It should be again pointed out that all conventionally fitted sets of parton densities are extrapolated to low- $x$  ( $x < 10^{-5}$ ) beyond the validity of the fitted parametrizations at  $x \gtrsim 10^{-5}$  using either some 'reasonable' analytic functions<sup>3</sup> [24, 25] or, in most cases, a fixed slope of  $x\bar{q}(x, M_W^2)$  at the lowest  $x$  permitted by present HERA experiments ( $x \simeq 10^{-5}$ ). As already demonstrated in fig. 1, the dynamical GRV 94 densities result in very similar high energy predictions as the GRV 98 ones, with GRV 94 cross sections being about 5 to 10% larger for  $E_\nu \gtrsim 10^9$  GeV. This is due to the fact that the GRV 94 sea and gluon densities are slightly steeper at small- $x$  than the GRV 98 ones. Notice that such a difference is within the typical uncertainty of about 20% at  $x \simeq 10^{-8}$  due to factorization scale ambiguities [15]. The same holds true for the results in fig. 4 based on the CTEQ4-DIS densities as used and extrapolated by GQRS 98 [6] and the CTEQ3-DIS distributions [24] which provide equally reasonable and acceptable



estimates of total neutrino cross sections [2], except perhaps at highest energies where GQRS 98(CTEQ4-DIS) possibly slightly underestimates them. The situation changes if we turn to the results based on the remaining extrapolated parton parametrizations in fig. 4: The FMR [1] extrapolations and the fixed-power extrapolated [2] MRS-G distributions [27] result in noticeably larger cross sections, up to almost a factor of 2, at large energies as compared to our dynamical QCD extrapolations and predictions. On the other hand, the EHLQ-DLA distributions [28], extrapolated [2] to  $x < 10^{-4}$  using the 'double logarithmic approximation' (DLA), strongly underestimate the cross sections almost throughout the whole high-energy range shown in fig. 4.

These results indicate that UHE (anti)neutrino nucleon total cross sections can be calculated with an uncertainty of about  $\pm 20\%$  at highest neutrino energies of  $10^{12}$  GeV which requires a reliable knowledge of parton distributions at  $x = 10^{-8}$  to  $10^{-9}$  and  $Q^2 = M_W^2$  [15]. This is considerably more accurate than the estimated uncertainty factor of  $2^{\pm 1}$  derived from ad hoc extrapolations of fitted parton distributions to very small- $x$  beyond the region of their validity [2, 6]. Thus all recent estimates of cosmic UHE neutrino event rates [2, 3, 4, 6] based on the dynamical GRV densities [13, 14, 15] and the properly extrapolated CTEQ distributions [24, 25], or parton densities with an effective similar small- $x$  behavior, appear to be realistic and accurate to within 20%; this is in contrast to estimates based on extrapolated versions of FMR [1] and MRS-G [2, 4] or MRS-D' [6] distributions, for example, which result in too large rates at highest neutrino energies of about  $10^{21}$  eV. These conclusions hold of course mainly for downward event rates, since the upward muon event rates are obviously rather insensitive to the particular choice of parton distributions due to the compensating attenuation of neutrinos as they pass through the Earth [2, 6].

## Acknowledgements

This work has been supported in part by the 'Bundesministerium für Bildung, Wissenschaft, Forschung und Technologie', Bonn.

## References

- [1] G.M. Frichter, D.W. McKay and J.P. Ralston, Phys. Rev. Lett. 74 (1995) 1508;  
J.P. Ralston, D.W. McKay and G.M. Frichter, 'The UHE Neutrino-Nucleon Cross Section', talk given at the *7th Intern. Symp. on Neutrino Telescopes*, Venice, Italy, Feb. 1996 ([astro-ph/9606008](#)).
- [2] R. Gandhi, C. Quigg, M.H. Reno and I. Sarcevic, Astropart. Phys. 5 (1996) 81.
- [3] G. Parente and E. Zas, Proc. of the *7th Intern. Symp. on Neutrino Telescopes*, Venice, Italy, Feb. 1996, p. 499 ([astro-ph/9606091](#));  
K.S. Capelle, J.W. Cronin, G. Parente and E. Zas, Astropart. Phys. 8 (1998) 321.
- [4] G.C. Hill, Astropart. Phys. 6 (1997) 215.
- [5] H1 collab.: I. Abt *et al.*, Nucl. Phys. B407 (1993) 515; T. Ahmed *et al.*, *ibid.* B439 (1995) 471; S. Aid *et al.*, Phys. Lett. B354 (1995) 494;  
ZEUS collab.: M. Derrick *et al.*, Phys. Lett. B316 (1993) 412; Z. Phys. C65 (1995) 379; Phys. Lett. B345 (1995) 576.
- [6] R. Gandhi, C. Quigg, M.H. Reno and I. Sarcevic, FERMILAB-PUB-98/087-T ([hep-ph/9807264](#)).
- [7] H1 collab.: S. Aid *et al.*, Nucl. Phys. B470 (1996) 3; C. Adloff *et al.*, *ibid.* B497 (1997) 3;  
ZEUS collab.: M. Derrick *et al.*, Z. Phys. C69 (1996) 607; *ibid.* C72 (1996) 399.
- [8] R.J. Protheroe, Univ. Adelaide ADP-AT-96-15, talk presented at Erice, Italy, June 1996 ([astro-ph/9612213](#)), and references therein; M. Roy and H.J. Crawford, 'Sources of UHE Neutrinos', LBL Berkeley report ([astro-ph/9808170](#)), and references therein.
- [9] K. Mannheim, Astropart. Phys. 3 (1995) 295;  
F. Halzen and E. Zas, Astrophys. J. 488 (1997) 669;

- R.J. Protheroe, 'High energy Neutrinos from Blazars' ([astro-ph/9607165](#)), in *Accretion Phenomena and Related Outflows*, ASP Conf. Series, vol. 121 (1997).
- [10] E. Waxman and J. Bahcall, Phys. Rev. Lett. 78 (1997) 2292; IAS Princeton report ([hep-ph/9807282](#));  
F. Halzen and G. Jaczko, Univ. Wisconsin MADPH-96-929.
- [11] R.J. Protheroe and T. Stanev, Phys. Rev. Lett. 77 (1996) 3708; 78 (1997) 3420 (E).  
G. Sigl, S. Lee, D.N. Schramm and P. Coppi, Phys. Lett. B392 (1997) 129;  
U.F. Wichoski, J.H. MacGibbon and R.H. Brandenberger, BROWN-HET-1115 ([hep-ph/9805419](#)).
- [12] M. Glück, E. Reya and A. Vogt, Z. Phys. C48 (1990) 471.
- [13] M. Glück, E. Reya and A. Vogt, Z. Phys. C53 (1992) 127; Phys. Lett. B306 (1993) 391.
- [14] M. Glück, E. Reya and A. Vogt, Z. Phys. C67 (1995) 433.
- [15] M. Glück, E. Reya and A. Vogt, DO-TH 98/07, WUE-ITP-98-019 ([hep-ph/9806404](#)), to appear in Eur. Phys. J. C.
- [16] H1 collab., papers 260 and 275, submitted to the *Int. Europhysics Conf. on HEP*, Jerusalem, August 1997;  
ZEUS collab., papers N-646 and N-647, *ibid*.
- [17] Particle Data Group, R.M. Barnett *et al.*, Phys. Rev. D54 (1996) 1.
- [18] M. Glück, S. Kretzer and E. Reya, Phys. Lett. B380 (1996) 171; B405 (1997) 391 (E).
- [19] M. Glück, R.M. Godbole and E. Reya, Z. Phys. C38 (1988) 441; C39 (1988) 590 (E).
- [20] W. Furmanski and R. Petronzio, Z. Phys. C11 (1982) 293.
- [21] T. Gottschalk, Phys. Rev. D23 (1981) 56.

- [22] T. Stelzer, Z. Sullivan and S. Willenbrock, Phys. Rev. D56 (1997) 5919.
- [23] M. Glück, E. Reya and M. Stratmann, Nucl. Phys. B422 (1994) 37.
- [24] H.L. Lai *et al.*, CTEQ3, Phys. Rev. D51 (1995) 4763.
- [25] H.L. Lai *et al.*, CTEQ4, Phys. Rev. D55 (1997) 1280.
- [26] T. Ahmed *et al.*, H1 collab., Phys. Lett. B324 (1994) 241; D. Haidt, Proceedings of the *3rd Tallinn Symposium on Neutrino Physics*, Lohusalu, Estonia, Oct. 1995, eds. I. Ots *et al.*, Tartu 1995, p. 7.
- [27] A.D. Martin, R.G. Roberts and W.J. Stirling, Phys. Lett. B354 (1995) 155.
- [28] E. Eichten, I. Hinchliffe, K. Lane and C. Quigg, Rev. Mod. Phys. 56 (1984) 579; *ibid.* 58 (1986) 1065 (E).

## Figure Captions

**Fig. 1** The light quark sea and gluon distributions in NLO at  $Q = M_W^2$ . The dynamical GRV 94 [14] and GRV 98 [15] predictions have been obtained from evolving the respective valence-like input at  $Q^2 = Q_0^2$  which is shown for illustration for the GRV 98 densities by the two curves at  $Q_0^2 = 0.40 \text{ GeV}^2$ . For comparison, the extrapolations of the CTEQ3 [24] and CTEQ4 [25]<sup>3</sup> distributions are shown as well.

**Fig. 2** Charged current  $\nu N$  cross sections as calculated in NLO. In the case of GRV 98 densities [15], heavy quark contributions are treated in a fully massive way based on fixed-order perturbation theory as explained in the text, whereas the GRV 92 distributions [13] refer to a massless (resummed) treatment of heavy quark flavors according to eq. (5). The GQRS 98 [6] calculation is based on the CTEQ4-DIS densities extrapolated to  $x < 10^{-5}$  using a fixed power in  $x$  as given at  $x = 10^{-5}$  and  $Q^2 = M_W^2$ ; this extrapolation method results in cross sections about 20 % larger at  $E_\nu = 10^{12} \text{ GeV}$  than the CTEQ4-DIS densities [25]<sup>3</sup> shown in fig. 1. The HERA measurement is taken from ref. [26].

**Fig. 3** The dependence of  $\sigma_{CC}^{\nu N}$  on the small- $x$  region, i.e. on the lower integration limit  $x_{min} \leq x$  in eq. (1), using the NLO GRV 98 parton distributions [15].

**Fig. 4** Ratio of charged current cross sections using different parton distribution functions (PDF) as compared to the GRV 98 distributions [15]. The PDF refer to GRV 94 [14], GQRS 98 (CTEQ4-DIS) [6], GQRS 96 (CTEQ3-DIS, MRS-G) [2], FMR [1] and EHLQ-DLA [2].

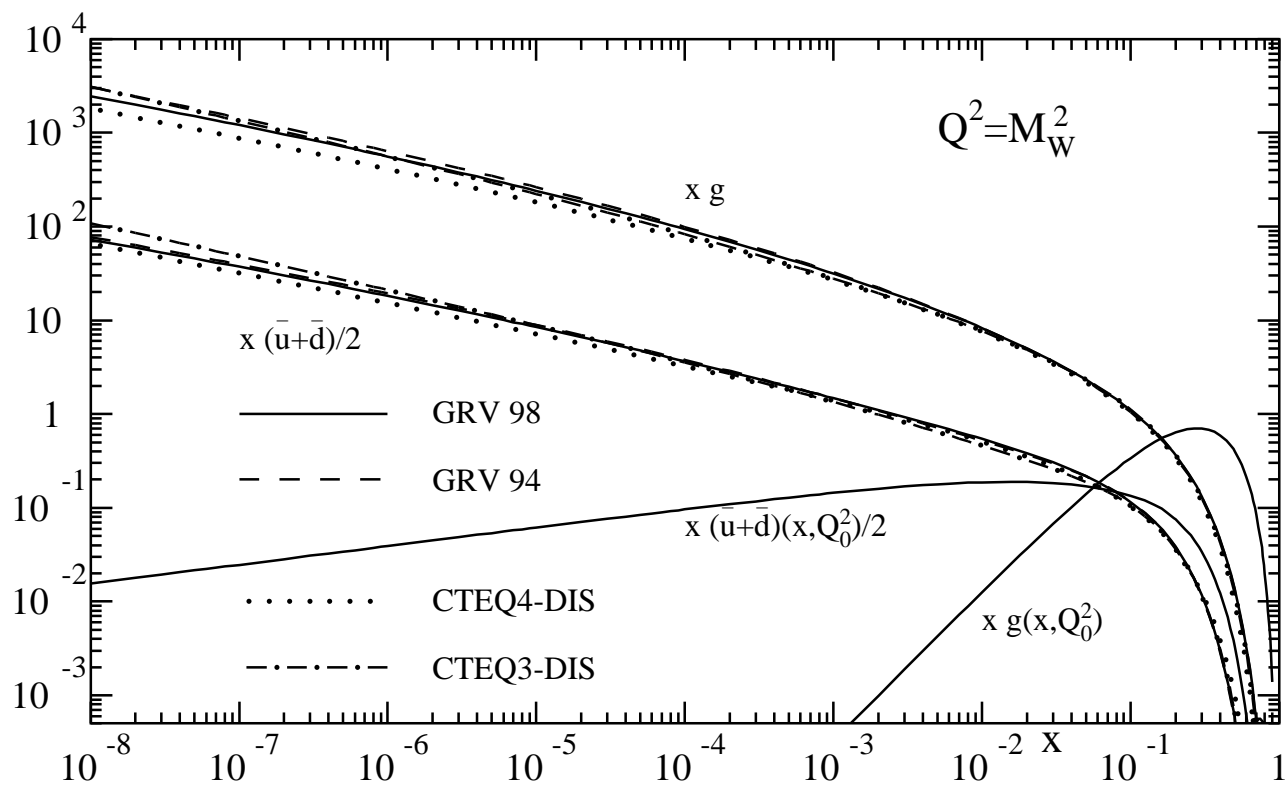


Fig. 1

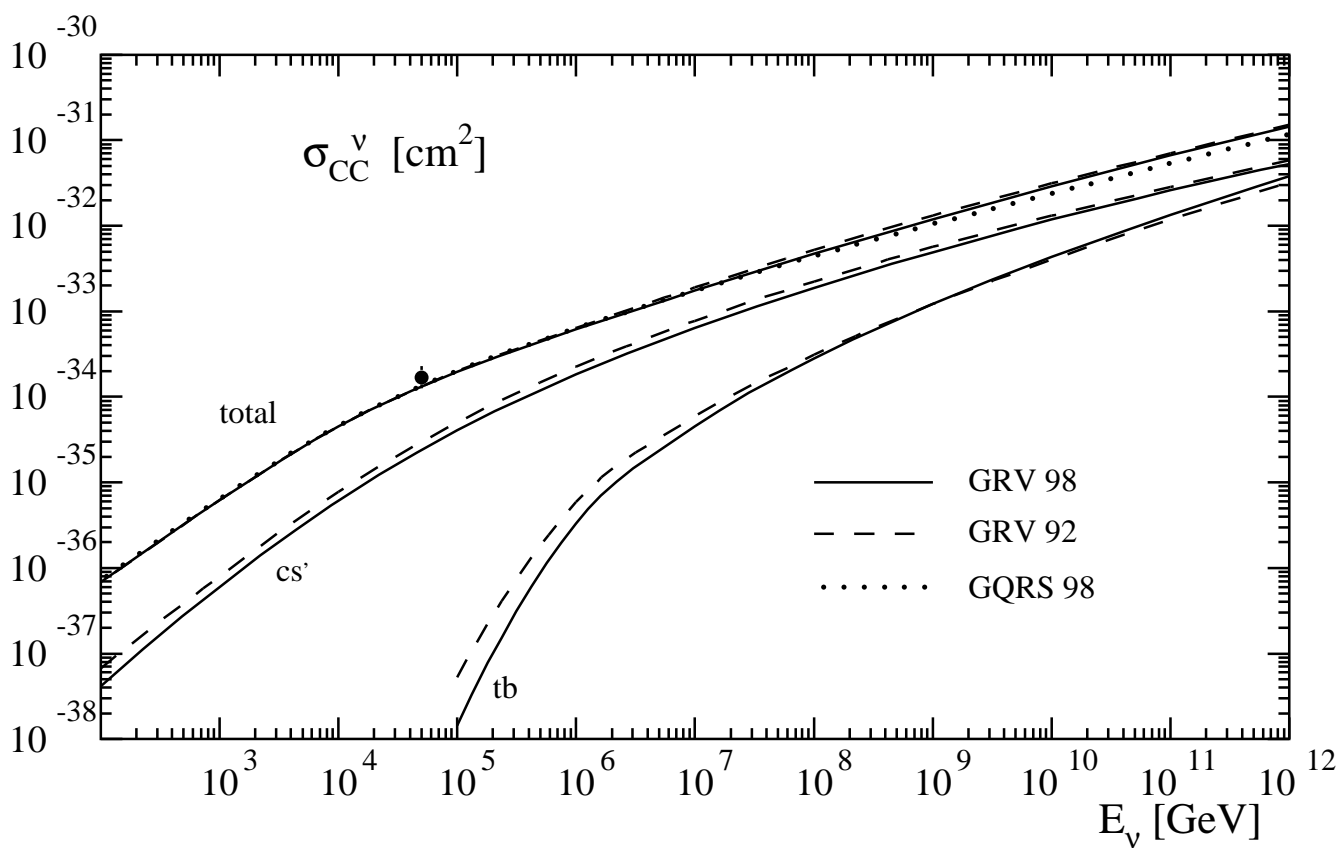


Fig. 2

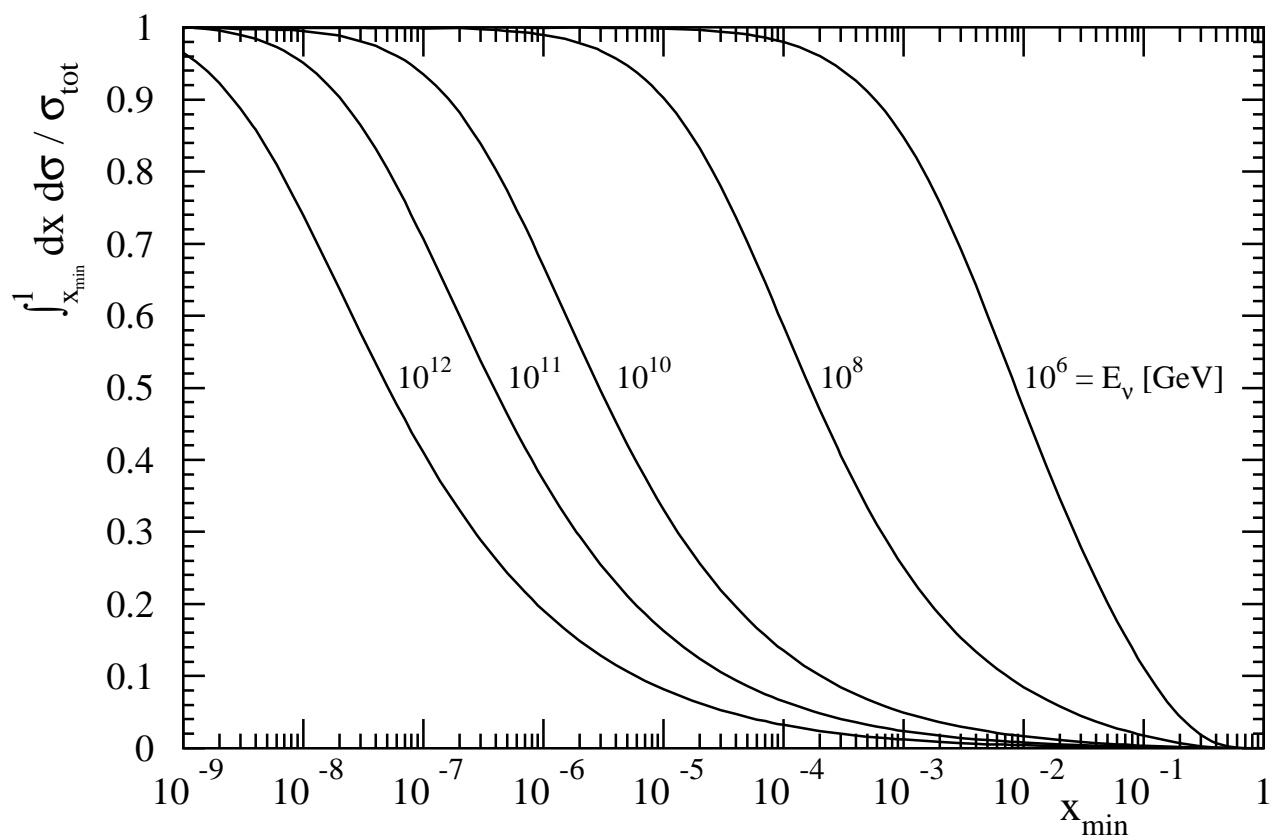


Fig. 3



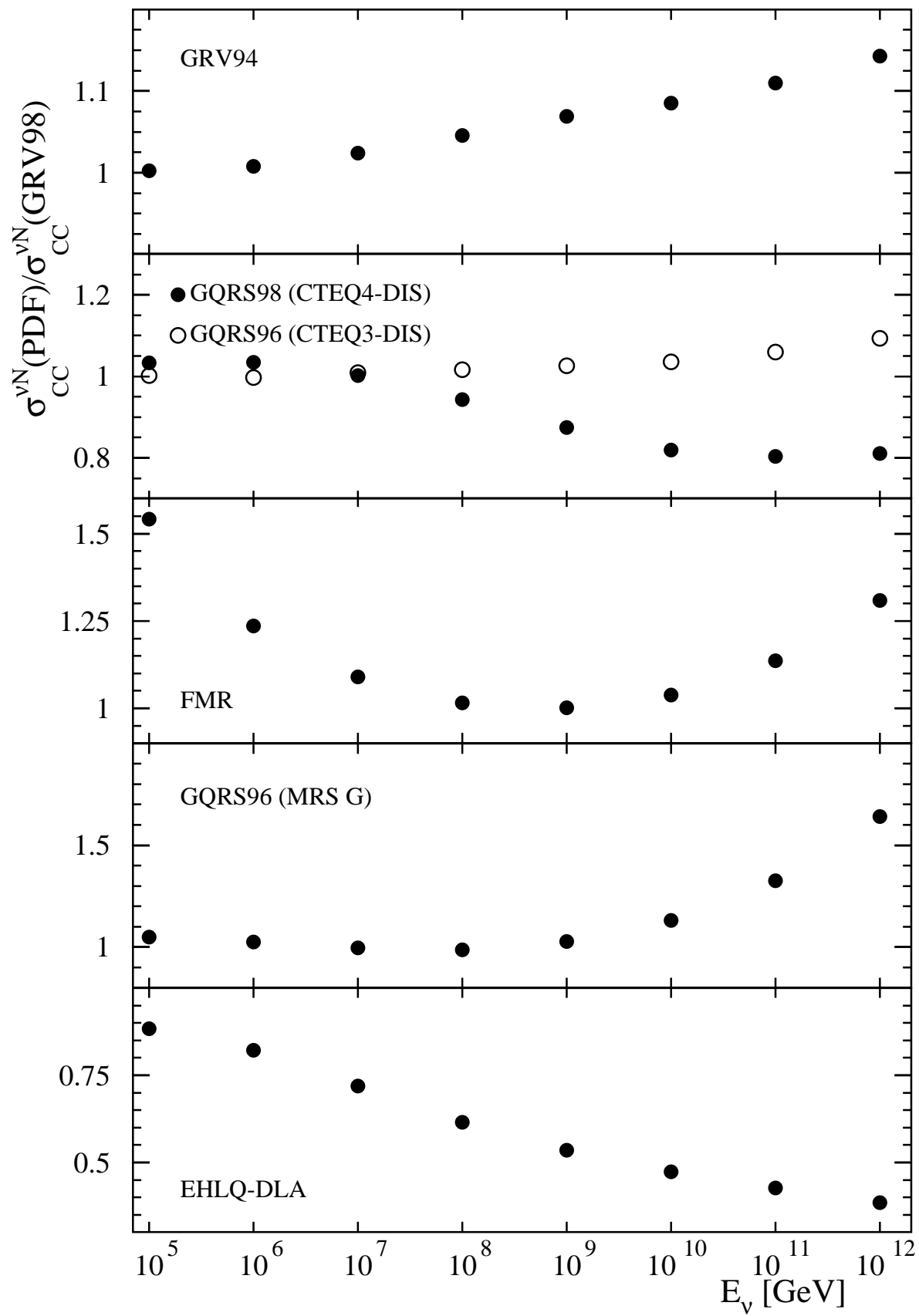


Fig. 4